408 *KSME International Journal, Vol. 14, No. 4, pp. 408~417, 2000*

Design and Simulation of Meshing of New Type of Worm-Gear Drive with Localized Contacts

Inhwan Seol*, Soonbae Chung
Senior Researcher, Agency for Defence Development

The design and simulation of meshing of a single enveloping worm-gear drive with modified surfaces is presented. Generally worm-gear is generated by the hob which is identical to the worm. This process guarantees the conjugation between the worm and the gear but results in a line contact at every instant which is very sensitive to misalignment. The localization of bearing contact is necessary to reduce the sensitivity of the worm-gear drive to misalignment. Practically this localization is achieved by application of an oversized worm type hob to cut the worm-gear. The oversized hob approach is very practical and effective to localize bearing contact but can not provide the conjugation between the worm and the modified worm-gear. This work proposes an analytical procedure to make the worm surface conjugate to the worm-gear which is cut by the oversized hob. The developed computer program allows the investigation of the influence of misalignment on the shift of the bearing contact and the determination of the transmission errors, the contact ratio and the principle curvatures. The developed approach has been applied for ZK type of single-enveloping worm-gear drives and the developed theory is illustrated with a numerical example.

Key Words : Worm-Gear, Simulation of Meshing, Contact Ellipse

1. Introduction

The worm-gear drive is an essential device applied in transformation of motion between crossed axes due to large speed reduction and high load carrying capacity. This device is composed of a driving worm and a driven worm-gear. Worm-gear drives with cylindrical worms are categorized as ZA, ZN, ZI, ZK, ZF types according to the geometry type of the worm or cutting method (Litvin, 1994).

Theoretically, worm-gear is generated by the hob that is identical to the mating worm to be conjugated ant the worm-gear surfaces are in line contact. However, worm-gear manufacturers apply oversized hob cutters for longer tool life and good meshing condition of gear drives. In previous researches(Bair and Tsay, 1998; Colbourne, 1989; Dudley, 1954; Fang and Tsay, 1996a; Seol and Litvin, 1996; Simon, 1998) the localization of the bearing contact of a worm-gear drive has been achieved by application of an oversized hob provided with the same type of thread surface as the worm. The localization has been done in such a manner that a path of bearing contact was positioned across the worm-gear tooth surface. This approach is accompanied with parabolic type of transmission error which is advantageous to reduce the noise and vibration of gear drives. However, the worm and worm-gear surfaces are not conjugated. This means that the transmission error exist even in ideal assembly condition. Moreover, the level of transmission error depends on the magnitude of the oversize. Therefore, large amount of oversize means that the tool life is prolonged but high level of transmission error can occur which is sometimes unacceptable for meshing worm-gear drive. Conjuga-

* Corresponding Author,
E-mail : seolkoo@chollian.net ; **TEL** : +82-42-863-8553
Senior Reseacher, Agency for Defence Development, Cheong-gu Apt. #104-1505, Cheonmin-dong, Yuseong-gu, Taejeon 305-390, Korea. (Manuscript **Received** July 26, 1999; **Revised** January 26, 2000)

tion is not only a basic requirement for gearing but also provides relatively lower level of transmission error even if large amount of oversize is applied to the hob. Therefore, there is a need to provide the worm surface which is conjugated to the worm-gear cut by an oversized hob.

The main goal of this paper is the development of a new type of conjugated worm and worm-gear surfaces with a localized bearing contact and reduced level of transmission error. This required novel application of the existing theory of gearing and its extension for the modified design and manufacture of worm-gear drives. The developed theory has been applied to ZK type of cylindrical worm-gear drive and well as a new K type of cylindrical worm-gear drive. The conventional K worm surface is not a ruled surface, but an envelope to the family of cone (grinding wheel) surfaces. Such a family of surface is generated by a surface of cone that performs a screw motion about the axis of the worm.

In this work a new approach with the following features is proposed:

(1) The thread surface of the worm and the oversized hob are designed as conjugated helical gears being in internal tangency

(2) The generated worm-gear and the worm are in point contact at every instant and the transformation of rotation is free of transmission error for an aligned worm-gear drive. Zero transmission error is provided for any magnitude of the oversize.

(3) The sensitivity of the worm-gear drive to errors of alignment is substantially reduced. The conjugation of the hob and the worm is based on the following ideas:

(i) The worm and the hob are considered as two helical gears that are simultaneously in mesh with two imaginary racks that have the same normal section (Fig. 1).

(ii) We may imagine that the hob and the worm perform rotational motions about their crossed axes (Fig. 2), and the shortest distance between the axes is determined by the equation

$$\Delta r = r_{ph} - r_{pw} \tag{1}$$

The crossing angle is determined by the equation

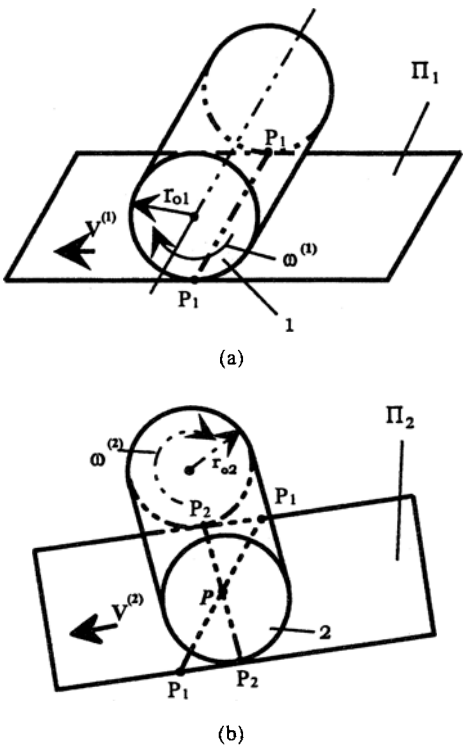

Fig. 1 Schemaic generation of conjugated tooth surfaces for helical gears with crossed axes

$$\Delta\gamma = \lambda_{ph} - \lambda_{pw} \tag{2}$$

Here, r_{ph} and r_{pw} are pitch radii of the hob and the worm, respectively. λ_{ph} and λ_{pw} are lead angles of the hob and the worm, respectively.

(iii) The two racks that are in simultaneous mesh with the hob and the worm perform related translational motions while the hob and the worm are rotated about their axes. The current displacement of both racks in the normal direction is the same. The normal direction is considered in the plane II that is tangent to the worm and the hob pitch cylinders at point P.

(iv) We remind that a helical gear and the respective rack have an instantaneous axis of rotation that is the generatrix of the helical gear (Fig. 1). There are two such instantaneous axes of rotation while the hob and the worm are in mesh with the two respective racks. These axes lie in plane II and intersect each other at point P.

(v) Considering the meshing of the hob and

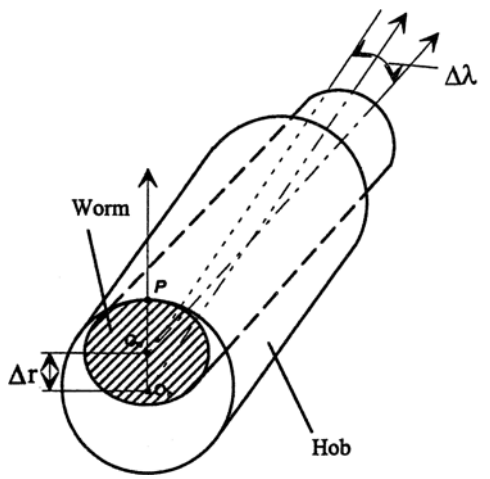

Fig. 2 Pitch cylinders of the worm and oversized hob

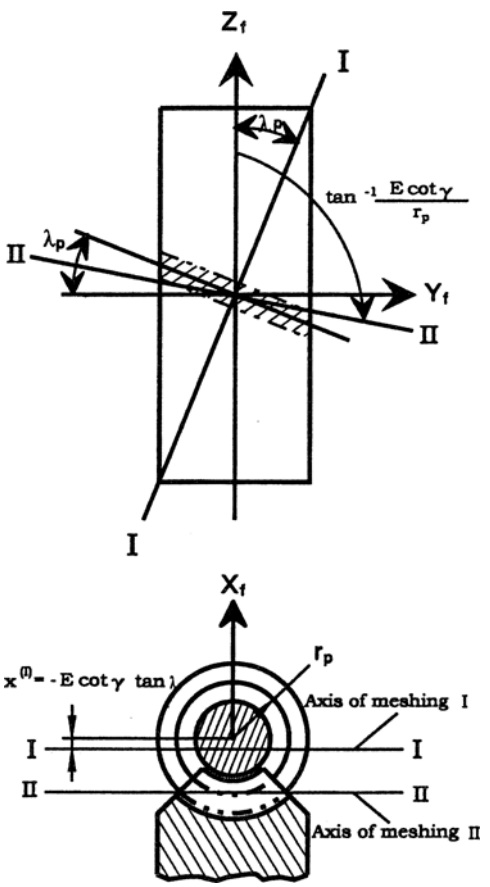

Fig. 3 Axes of meshing in non-orthogonal worm-gear drive

the worm-gear being generated, we have to recognize that the hob and the worm-gear are in a line contact and there are two axes in meshing, $I-I$ and $II-II$, that represent two crossed straight lines (Fig. 3). We require that point P shown in Fig. 1 belongs to the axis of meshing $II-II$ (Fig. 3).

(vi) The discussed conditions, if observed, provide that the surfaces of the worm and the generated worm-gear are in point contact at every instant, the contact is localized, and the transmission function is linear with respect to the prescribed gear ratio.

It will be shown below that the bearing contact is localized in the middle of the worm-gear tooth surface. Errors of alignment cause negligible transmission errors. However, the magnitude of alignment errors must be limited to avoid impermissible shift of bearing contact.

2. Generation of Hob Surfaces

The hob surface is generated by a conical shaped grinding wheel (Seol and Litvin, 1996). The surface of the hob is generated by the cone which performs a screw motion with respect to the hob (Fig. 4). The cutting planes of the cone is installed in the normal section of the hob, that is, the cone axis forms an angle λ_p with the hob axis. λ_p is the lead angle on the pitch cylinder of the hob. By modelling the process of generation, the hob surfaces are represented in two parametric forms. After skipping the detailed procedure of generation, the final expressions of the K type of helicoid surface for a right handed hob and its surface normal are as follows

$$x_h = u_c(\cos\alpha_c\cos\theta_c\cos\psi_c + \cos\alpha_c\cos\gamma_c\sin\theta_c\sin\psi_c - \sin\alpha_c\sin\gamma_c\sin\psi_c) + \alpha\sin\gamma_c\sin\psi_c + E_c\cos\psi_c \quad (3)$$

$$y_h = u_c(-\cos\alpha_c\cos\theta_c\sin\psi_c + \cos\alpha_c\cos\gamma_c\sin\theta_c\cos\psi_c - \sin\alpha_c\sin\gamma_c\cos\psi_c) + \alpha\sin\gamma_c\cos\psi_c - E_c\sin\psi_c \quad (4)$$

$$z_h = u_c(\sin\alpha_c\cos\gamma_c + \cos\alpha_c\sin\gamma_c\sin\theta_c) - p\psi_c - \alpha\cos\gamma_c \quad (5)$$

$$n_{hx} = \cos\psi_c\sin\alpha_c\cos\theta_c + \sin\psi_c(\cos\gamma_c\sin\alpha_c\sin\theta_c + \sin\gamma_c\cos\alpha_c) \quad (6)$$

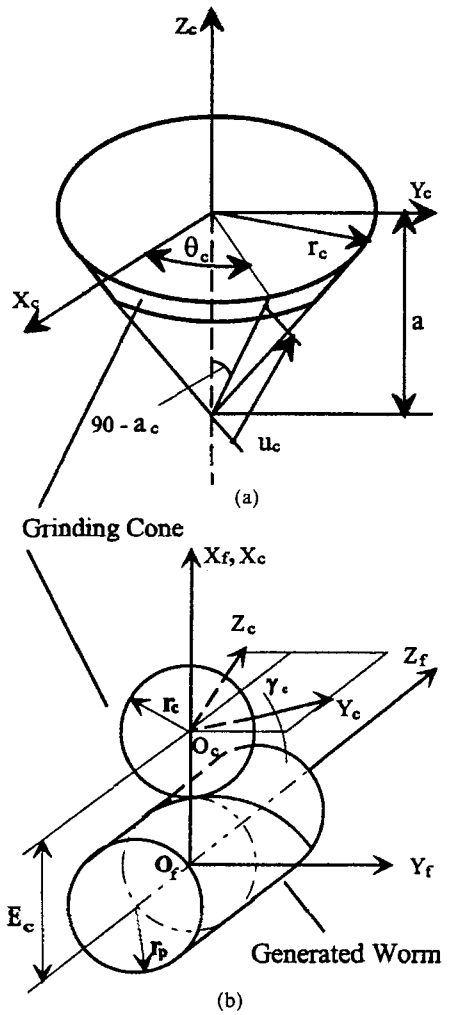

Fig. 4 Grinding cone and its installation for generation of ZK type of worm surfaces

$$n_{hy}=-\sin\phi_c\sin\alpha_c\cos\theta_c+\cos\phi_c(\cos\gamma_c\sin\alpha_c\sin\theta_c+\sin\gamma_c\cos\alpha_c) \quad (7)$$

$$n_{hz}=\sin\gamma_c\sin\alpha_c\sin\theta_c-\cos\gamma_c\cos\alpha_c \quad (8)$$

where

$$u_c=a\sin\alpha_c-(E_c\sin\alpha_c\cot\gamma_c+p\sin\alpha_c)\tan\theta_c-(E_c-p\cot\gamma_c)\cos\alpha_c/\cos\theta_c \quad (9)$$

where u_c, θ_c and ϕ_c are surface parameters, and α_c is the pressure angle and γ_c is the installing angle of the cone and E_c is the shortest center distance between the cone and the hob.

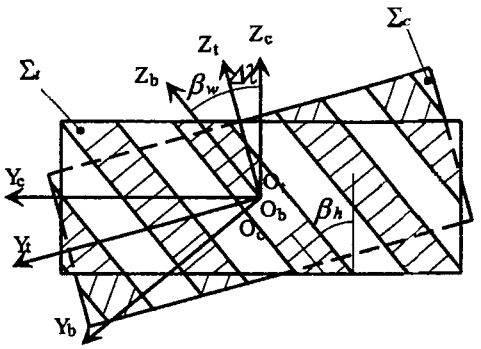

Fig. 5 Two rack-cutters

3. Some Considerations for the Conjugation of the Worm

A method for the generation of the conjugate surface of the worm is based on the following considerations.

(1) The given hob surface $\sum_h$ generates the surface of the rack-cutter surface $\sum_c$.

(2) Another rack-cutter $\sum_t$ is used for the generation of the surface of the worm. Surfaces $\sum_c$ and $\sum_t$ of the rack-cutters are provided with coinciding planes and their orientation is shown in Fig. 5. Both generating rack cutters have the same normal section. However the orientations of $\sum_c$ and $\sum_t$ are different and are determined by the directions and magnitudes of the helix (or lead) angles β_{pi} $(i=1, 2)$ of the worm and the oversized hob (Fig. 5).

(3) In the process of generation the worm and the hob perform constant rotational motions and the respective rack-cutters perform the related translational motion.

(4) Surfaces $\sum_h$ and $\sum_c$ are in line contact at every instant. Surfaces $\sum_t$ and $\sum_w$ are also in a line contact at every instant. These two lines of contact are intersected and this intersected point is the common tangent point of the hob and the worm.

(5) If K-helicoid is used for the surface of the hob, then the generated surface of the worm is not a K-helicoid but another helicoid.

Figure 6 shows the location and the orientation of the hob, rack-cutters, and worm with respect to each other. Coordinate systems S_m and S_n are the

fixed ones used to describe the generation of the rack and the worm. The Z_m and Z_n axes are the rotation axes of the worm and the oversized hob, respectively. These axes form the crossing angle $\Delta\lambda$ and the shortest distance Δr ; Δr and $\Delta\lambda$ depend on the chosen oversize that affects the deepness of the localization.

Movable coordinate systems S_h and S_w are rigidly connected to the oversized hob and the worm, respectively (Fig. 6). The hob and the worm perform rotation about their axes, and the angles of rotation are designated by ϕ_c and ϕ_t. Movable coordinate systems S_c and S_t are rigidly connected to the rack-cutters and perform translational motions while the hob and the worm rotate. The directional vectors of the translation of racks are on the planes perpendicular to the rotation axes of the hob and the worm, respectively.

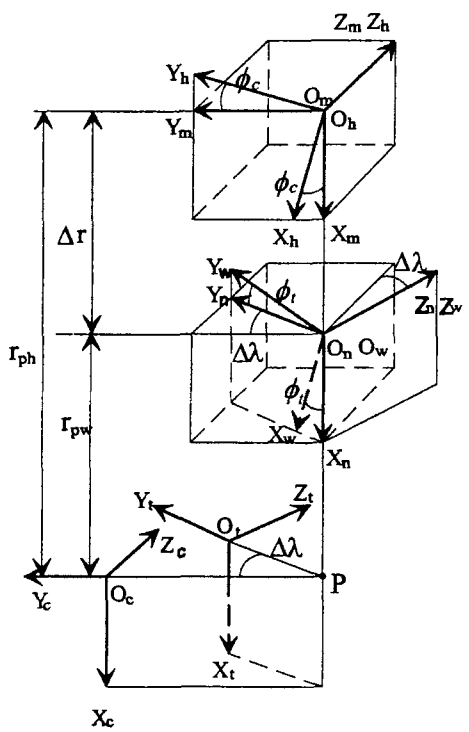

Fig. 6 Applied coordinate systems for determination of conjugated worm

4. Determination of the Surface of the Rack Conjugated to the Oversized Hob

4.1 Meshing of the K-Hob with a rack

The surface of the hob is considered as given to be a K-helicoid with a predetermined oversize. The K-helicoid surface has been already derived in the previous section and represented in two-parameter form as follows

$$r_h = r_h(\theta, \zeta) \tag{10}$$

$$n_h = \frac{N_h}{|N_h|},\ N_h = \frac{\partial r_h}{\partial \theta} \times \frac{\partial r_h}{\partial \zeta} \tag{11}$$

We may consider the meshing of a K-helicoid hob $\sum_h$ with the rack $\sum_c$ in plane $Z_h=0$ that is perpendicular to the Z_h axis. The derivation of the tooth surface $\sum_c$ of the rack is represented as the determination of the envelope to the family of the hob surface (K-helicoid).

The hob and the rack perform rotational and translational motions, respectively. These two motions are related as

$$v_c = r_{ph}\omega_h \tag{12}$$

Here, r_{ph} is the radius of the pitch cylinder of the hob ; ω_h is the angular velocity of the hob ; v_c is the linear velocity of the rack (Fig. 7). The instantaneous axis of rotation, $I_h - I_h$, is parallel to the hob axis and is represented in S_m as

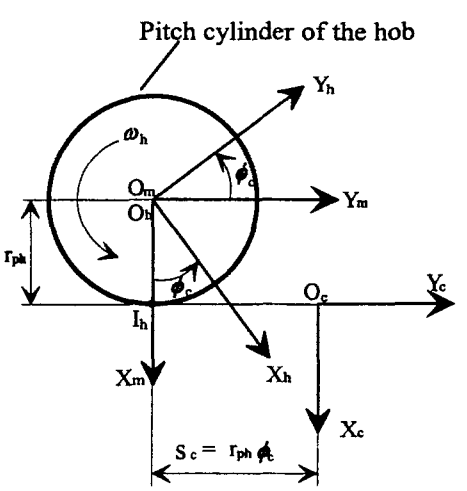

Fig. 7 Determination of the rack conjugated to the oversized hob

$$[X_m \ Y_m \ Z_m]^T=[r_{ph} \ 0 \ l]^T \tag{13}$$

where (X_m, Y_m, l) determine a current point of I_h-I_h ; l is a varied parameter.

The instantaneous axis of rotation is represented in S_h by the following matrix equation

$$[X_h \ Y_h \ Z_h]^T=M_{hm}[X_m \ Y_m \ Z_m]^T \tag{14}$$

where

$$M_{hm}=\begin{bmatrix} \cos\phi_c & \sin\phi_c & 0 & 0 \\ -\sin\phi_c & \cos\phi_c & 0 & 0 \\ 0 & 0 & 1 & 0 \\ 0 & 0 & 0 & 1 \end{bmatrix} \tag{15}$$

Equations (14) and (15) yield

$$[X_h \ Y_h \ Z_h]^T=[r_{ph}\cos\phi_c \ r_{ph}\sin\phi_c \ l]^T \tag{16}$$

4.2 Equation of meshing

Derivation of equation of meshing is based on the consideration that the normal to $\sum_h$ determined at any point of the line of contact between $\sum_h$ and $\sum_c$ passes through the instantaneous axis of rotation I_h-I_h(Gu, 1997). Thus, we have

$$\frac{X_h-x_h(\theta, \zeta)}{n_{xh}(\theta, \zeta)}=\frac{Y_h-y_h(\theta, \zeta)}{n_{yh}(\theta, \zeta)} =\frac{Z_h-z_h(\theta, \zeta)}{n_{zh}(\theta, \zeta)} \tag{17}$$

Taking into account the relation $n_x y-n_y x=p\, n_z$ obtained for a helicoid and using Eq. (16) and (17), we may derive the equation of meshing as

$$f_{hc}(\theta, \zeta, \phi_c)=(n_{yh}\cos\phi_c+n_{xh}\sin\phi_c)\, r_{ph} -p_h n_{zh}=0 \tag{18}$$

where ϕ_c is the generalized parameter of motion represented as the angle of rotation of the hob.

4.3 Determination of the rack surface $\sum_c$

The surface of rack $\sum_c$ is represented by the following equations

$$r_c(\theta, \zeta, \phi_c)=M_{ch}r_h(\theta, \zeta) \tag{19}$$
$$n_c(\theta, \zeta, \phi_c)=L_{ch}n_h(\theta, \zeta) \tag{20}$$
$$f_{hc}(\theta, \zeta, \phi_c)=0 \tag{21}$$

where M_{ch} is the coordinate transformation matrix between coordinate systems S_c and S_h

Equations from (19) to (21) enable the representation of the rack surface $\sum_c$ as follows

$$r_c=\begin{bmatrix} \cos\phi_c x_h-\sin\phi_c y_h-r_{ph} \\ \sin\phi_c x_h+\cos\phi_c y_h-r_{ph}\phi_c \\ z_h \end{bmatrix} \tag{22}$$

$$n_c=\begin{bmatrix} \cos\phi_c n_{xh}-\sin\phi_c n_{yh} \\ \sin\phi_c n_{xh}+\cos\phi_c n_{yh} \\ z_{zh} \end{bmatrix} \tag{23}$$

5. Determination of the Worm Thread Surface Conjugated to the Rack Surface $\sum_t$

5.1 Surface of rack-cutter $\sum_t$ used for generation of worm surface

The rack surface $\sum_t$ is the same as $\sum_c$ but is represented in coordinate system S_t oriented with respect to $\sum_c$ according to the similar procedure to Fig. 8. Our goal is to determine the worm surface that is generated by $\sum_t$. The rack surface $\sum_t$ and its unit normal are represented in S_t by the following matrix equations

$$r_t(\theta, \zeta, \phi_c)=M_{tc}\, r_c(\theta, \zeta, \phi_c) \tag{24}$$
$$n_t(\theta, \zeta, \phi_c)=L_{tc}\, n_c(\theta, \zeta, \phi_c) \tag{25}$$
$$f_{hc}(\theta, \zeta, \phi_c)=0 \tag{26}$$

where, M_{tc} is the coordinate transformation matrix between coordinate systems S_c and S_t.

Eqs. (24) to (26) yield

$$r_t=\begin{bmatrix} x_c \\ \cos\Delta\lambda \ y_c-\sin\Delta\lambda \ z_c \\ \sin\Delta\lambda \ y_c+\cos\Delta\lambda \ z_c \end{bmatrix} \tag{27}$$

$$n_t=\begin{bmatrix} n_{xc} \\ \cos\Delta\lambda \ n_{yc}-\sin\Delta\lambda \ n_{zc} \\ \sin\Delta\lambda \ n_{yc}+\cos\Delta\lambda \ n_{zc} \end{bmatrix} \tag{28}$$

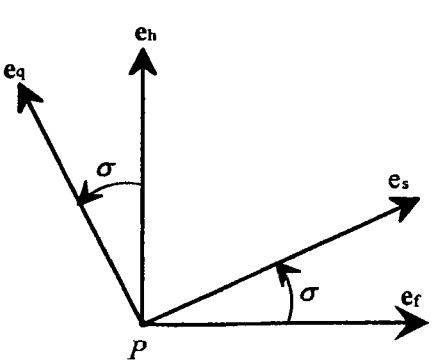

Fig. 8 Unit vectors in tangent plane

5.2 Meshing of rack $\sum_t$ with the worm

The worm and the rack perform rotational and translational motion, respectively. The same procedure as shown in Sec. 5 can be applied and the following equations for the worm surface $\sum_w$ and its unit normal are derived with two meshing equations

$$\mathbf{r}_w=\begin{bmatrix}\cos\phi_t x_t+\sin\phi_t y_h+r_{pw}\cos\phi_t+r_{pw}\phi_t\sin\phi_t\\-\sin\phi_t x_t+\cos\phi_t y_h-r_{pw}\sin\phi_t+r_{pw}\phi_t\cos\phi_t\\z_t\end{bmatrix} \tag{29}$$

$$\mathbf{n}_w=\begin{bmatrix}\cos\phi_t n_{xt}+\sin\phi_t n_{yt}\\-\sin\phi_t n_{xt}+\cos\phi_t n_{yt}\\n_{zt}\end{bmatrix} \tag{30}$$

6. Generation of Worm-Gear by Hob

The worm-gear tooth surface generated by the hob may be determined by simulation of meshing between the oversized hob and gear. The applied coordinate systems are shown in Fig. 9. Since the worm-gear tooth surface is the envelope to the family of hob surface $\sum_h$ in S_g, the surface and its unit normal may be represented as follows

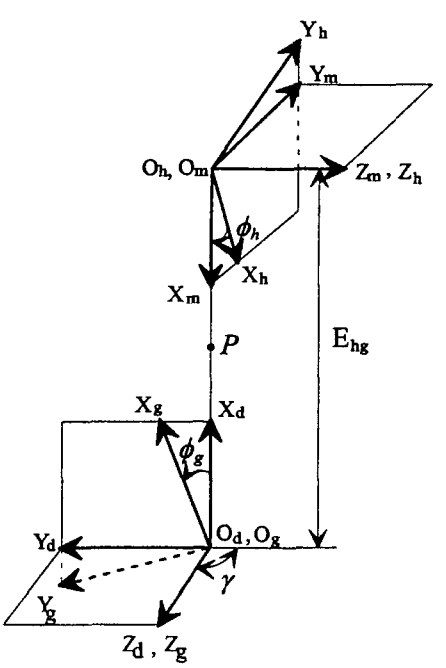

Fig. 9 Applied coordinate systems for generation of worm-gear

$$\mathbf{r}_g(\theta',\ \zeta',\ \phi_h)=\mathbf{M}_{gh}(\phi_h)\mathbf{r}_h(\theta',\ \zeta') \tag{31}$$

$$\mathbf{n}_g(\theta',\ \zeta',\ \phi_h)=\mathbf{L}_{gh}(\phi_h)\mathbf{n}_h(\theta',\ \zeta') \tag{32}$$

where $\mathbf{M}_{gh}$ is the coordinate transformation matrix from S_h to S_g and $\mathbf{L}_{gh}$ is the sub-matrix of $\mathbf{M}_{gh}$.

7. Determination of Contact Ellipse

7.1 Basic consideration

The bearing contact of the worm-gear drive forms a set of contact ellipses on the worm-gear surfaces. These contact ellipses are the analytical bases for the stress and lubrication analyses of contacting tooth surfaces. The determination of the instantaneous contact ellipse requires the knowledge of the principal curvatures and the principal directions at the point of tangency of the contacting surfaces.

Generally, since the generated surface is represented in three-parameter form with nonlinearly related parameters, it is very difficult to determine the principal curvatures and the directions of the surface by direct calculation (Litvin and Hsiao, 1993). Therefore, if the principal curvatures and directions of one surface are known, the direct relations between paincipal curvatures of the mating surfaces substantially simplify the determination of principal curvatures of the other surface.

This relation is applied to obtain the curvatures of worm-gear $\sum_g$ and worm $\sum_w$ as follows

(i) First, the principal curvatures and directions of hob $\sum_h$ should be determined by direct calculation.

(ii) Then using this relation, the principal curvatures and directions of worm-gear $\sum_g$ can be determined from the known hob $\sum_h$.

(iii) The principal curvatures and directions of the worm $\sum_w$ can be determined from the curvatures of rack $\sum_t$ that can be determined from the known hob $\sum_h$

This approach is based on the following ideas (Litvin and Kin, 1992):

(i) The velocity of a contact point in a fixed coordinate system is represented in two components ; (*a*) transfer motion with the surfaces ;

(b) relative motion over the surfaces

(ii) The displacement over the surface may be decomposed and represented by two components in separate motions along the principal directions of the respective surface.

7.2 Direct relations between princpal curvatures of mating surfaces

In Fig. 8 P is the point of tangency between surfaces $\sum_1$ $\sum_2$; $\mathbf{e}_f$ and $\mathbf{e}_h$ are the unit vectors of principal directions on $\sum_1$ at point P ; $\varkappa_s$ and $\varkappa_h$ are the respective principal curvatures of $\sum_1$; $\mathbf{e}_s$ and $\mathbf{e}_q$ represent the principal directions on $\sum_2$; $\varkappa_s$ and $\varkappa_q$ are the respective principal curvatures of $\sum_2$; angle σ is formed between $\mathbf{e}_f$ and $\mathbf{e}_s$ and measured counterclockwise from $\mathbf{e}_f$ to $\mathbf{e}_s$.

After skipping the very complicated derivation, we may obtain the following relations from the consideration that the displacement over the surface can be decomposed into two principal directions

$$\tan 2\sigma=\frac{2t_{13}t_{23}}{t_{23}^2-t_{13}^2-(\varkappa_f-\varkappa_h)t_{33}} \tag{33}$$

$$\varkappa_q-\varkappa_s=\frac{2t_{13}t_{23}}{t_{33}\sin 2\sigma} \tag{34}$$

$$\varkappa_q+\varkappa_s=\frac{\varkappa_f+\varkappa_h+t_{13}^2+t_{23}^2}{t_{33}} \tag{35}$$

Here

$$t_{13}=-(\omega^{(12)}\cdot\mathbf{e}_h)-\varkappa_f(\mathbf{v}^{(12)}\cdot\mathbf{e}_f) \tag{36}$$

$$t_{23}=(\omega^{(12)}\cdot\mathbf{e}_f)-\varkappa_h(\mathbf{v}^{(12)}\cdot\mathbf{e}_h) \tag{37}$$

$$t_{33}=-\mathbf{n}\cdot[\omega^{(1)}\times\mathbf{v}_{tr}^{(2)}-\omega^{(2)}\times\mathbf{v}_{tr}^{(1)}]+(\omega_1)^2m'_{21}(\mathbf{n}\times\mathbf{k}_2)\cdot(\mathbf{r}_1-\mathbf{R})+(\mathbf{n}\times\omega^{(12)})\cdot\mathbf{v}^{(12)}-\varkappa_f(v_f^{(12)})^2-\varkappa_h(v_h^{(12)})^2 \tag{38}$$

Here $v_f^{(12)}=\mathbf{v}^{(12)}\cdot\mathbf{e}_f$ and $v_h^{(12)}=\mathbf{v}^{(12)}\cdot\mathbf{e}_h$.

Equations (33) to (38) can provide the opportunity to determine the principal curvatures and directions on surface $\sum_2$ knowing the principal curvatures and directions on surface $\sum_1$ and parameters of motion of the interacting surfaces.

We may apply these equations to $\sum_h$ and $\sum_c$, $\sum_t$ and $\sum_w$, and $\sum_h$ and $\sum_g$, and then get curvatures of worm surface $\sum_w$ and worm-gear surface $\sum_g$. This means that if we only know the directions and magnitude of principal curvatures of $\sum_h$, we can determine the directions and magnitude of the principal curvatures of $\sum_w$ and $\sum_g$ without $\sum_w$ and $\sum_g$.

The orientation of the contact ellipse and its dimensions can be determined by the same procedures as shown by Litvin and Hsiao (1993).

8. Simulation of Meshing of the Worm and Worm-Gear Drive

8.1 Meshing and contact

We consider the meshing of the modified worm $\sum_w$ (provided with a conjugation to oversized hob $\sum_h$) with the worm-gear tooth surface $\sum_g$ that is generated by the hob $\sum_h$. The mismatch of $\sum_w$ with respect to the hob surface $\sum_h$ is required for the localization of the bearing contact between the worm and the worm-gear.

The simulation of meshing is based on the condition of continuous tangency of surfaces $\sum_w$ and $\sum_g$, that is performed by the tooth contact analysis.

The parameters that may be chosen for the initial contact can be obtained by considering that five surfaces — $\sum_c$, $\sum_t$, $\sum_h$, $\sum_w$ and $\sum_g$ — are in tangency at one point.

8.2 Numerical example

The computerized simulation of meshing was performed for a K-worm-gear drive with the following design parameters:

The investigation of results of simulation are as follows:

(i) Path of bearing contact exists across the worm-gear surface and locates around the center of the worm-gear surface (Fig. 10 and 12). Without misalignment, there is no transmission error as we expect (Fig. 11).

Table 1 Design parameters of worm and worm-gear

Number of Worm threads	$N_w=2$
Number of Gear Teeth	$N_g=30$
Axial Module	$m_{ax}=8.0\ mm$
Normal Pressure Angle	$\alpha_c=25°$
Shortest Center Distance	$E=176\ mm$
Magnitude of Oversize	$\Delta r=1.0\ or\ 4.0\ mm$

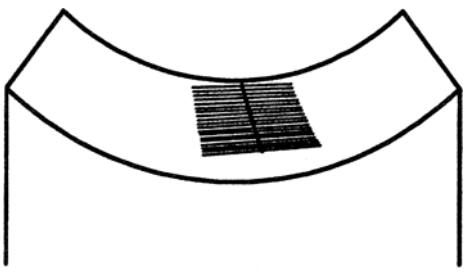

Fig. 10 Path of bearing contact with contact ellipses on ZK worm-gear surface : the amount of oversize, $\Delta r = 1.0$ mm, no misalignment

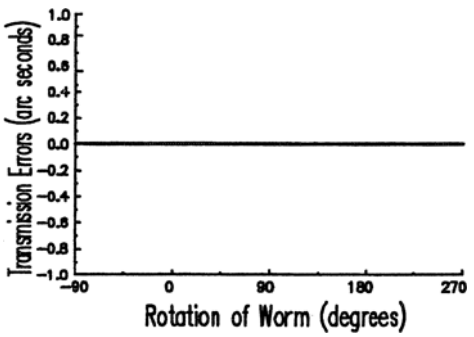

Fig. 11 Transmission error : the amount of oversize, $\Delta r = 1.0$ mm, no misalignment

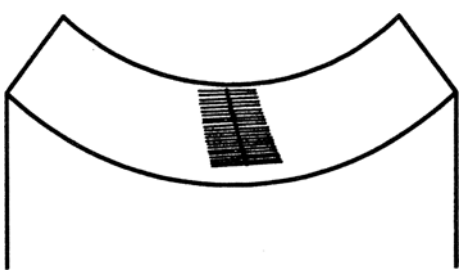

Fig. 12 Path of bearing contact with contact ellipses on ZK worm-gear surface : the amount of oversize, $\Delta r = 4.0$ mm, the error of center distance, 0.1 mm and the error of crossing angle, 3.0 arc min.

(ii) The greater the hob oversize, the contact ellipses of bearing contact become smaller, and the magnitude of the transmission error becomes larger but the location of the path of bearing contacts is almost the same (Fig. 10 to 13).

(iii) With practical misalignments, the transmission error is almost linear but its magnitude is within 1 arc. second. This level of transmission error is acceptible without any further modification (Fig. 13).

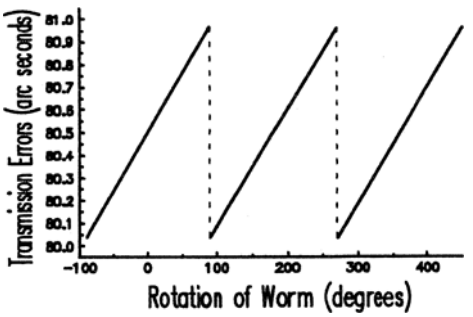

Fig. 13 Transmission error : the amount of oversize, $\Delta r = 4.0$ mm, the error of center distance, 0.1 mm and the error of crossing angle, 3.0 arc min.

(iv) The location of bearing contact and the sizes of contact ellipses are almost the same as in the case of the oversized hob approach. Therefore we can infer that the newly generated worm surface is not a K-helicoid but it deviates slightly from the original K-helicoid.

(v) If the level of transmission error is too high, then plunging method could be applied in worm-gear generation, which is expected to provide a parabolic function of transmission error.

9. Conclusion

From the above investigations, we can make the following conclusions

(1) The approach proposed in this work can provide very stable bearing contact for misaligned gear drives.

(2) Compared to the oversized hob approach, this approach is more theoretical and can provide stable point contact condition accommpanied with smaller transmission error for the same amount of misalignment.

(3) By adjusting the amount of oversize, we can make the bearing contact more appropriate according to the condition of application of gear drives.

(4) Computerized determination of the principal curvatures and directions of complex surfaces of a worm-gear and a worm represented by more than two but related surface parameters has been represented.

(5) This approach can be applied to various types of worm-gear drives such as ZA, ZN, ZI, and ZF worm-gear.

References

Bair, B. W. and Tsay, C. B., 1998, "ZK-Type Dual-Lead Worm and Worm-Gear Drives: Contact Teeth, Contact Ratio and Kinematic Errors," *ASME Journal of Mechanical Design*, Vol. 120, pp. 422~428.

Buckingham, E., 1963. "*Analytical Mechanics of Gears*," 2nd ed. Dover Publication.

Colbourne, J. R., 1989, "The Use of Oversize Hobs to Cut Worm Gears," AGMA paper 89FTB8.

Dudley, D. W., *Gear Handbook*. The Design, Manufacture, and Application of Gears. McGraw-Hill, NY, 1962.

Dudley, D. W., 1954. *Practical Gear Handbook*, McGraw-Hill, NY.

Gu, Inhoy, 1997, "Design of Antibacklash Pin Gearing," *KSME International Journal*, Vol. 11, No. 6, pp. 611~619.

Hong-Sheng Fang and Chung-Biau Tsay, 1996 (a), "Effects of the Hob Cutter Regrinding and Setting on ZE-Type Worm Gear Manufacture," *Int. J. Mach. Tools Manufact*. Vol. 36, No. 10, pp. 1123~1135.

Fang, H. S. and Tsay, C. B., 1996(b), "Mathematical Model and Bearing Contacts of the ZK-Type Worm Gear Set Cut by Oversize Hob Cutter," *Mechanism and Machine Theory*, Vol. 31, No. 3, pp. 271~282.

Litvin, F. L., 1994, *Gear Geometry and Applied Theory*. Prentice Hall NJ.

Litvin, F. L. and Hsiao, C. L, 1993, "Computerized Simulation of Meshing and Contact of Enveloping Gear Tooth Surfaces," *Computer Methods in Applied Mechanics and Engineering*.

Litvin, F. L. and Kin. V., 1992, "Computerized Simulation of Meshing and Bearing Contact for Single-Enveloping Worm-Gear Drives," *ASME Journal of Mechanical Design*. Vol. 114, pp. 313~316.

Litvin, F. L., Kin, V. and Zhang, Y., 1990, "Limitations of Conjugate Gear Tooth Surfaces," *ASME Journal of Mechanical Design*. Vol. 112, pp 230~236.

Seol, I. H. and Litvin, F. L., 1996, "Computerized Design, Generation and Simulation of Meshing and Contact of Modified Involute, Klingelnberg and Flender Type Worm-Gear Drives," *ASME Journal of Mechanical Design*. Vol. 118, pp. 551~555.

Simon, V. V., 1998, "Characteristics of a New Type of Cylindrical Worm Gear Drive," *ASME Journal of Mechanical Design*. Vol. 120, pp. 139~146.